Experimental Demonstration of a 43-dBi Gain Transmitarray in PCB Technology for Backhauling in the 300-GHz Band

Orestis Koutsos, Francesco Foglia Manzillo, Mathieu Caillet, Ronan Sauleau, Antonio Clemente

Experimental Demonstration of a 43-dBi Gain Transmitarray in PCB Technology for Backhauling in the 300-GHz Band

Orestis Koutsos, Francesco Foglia Manzillo, *Member, IEEE,* Mathieu Caillet, Ronan Sauleau, *Fellow, IEEE* and Antonio Clemente, *Senior Member, IEEE,*

***Abstract*—In this paper, a low-cost transmitarray antenna, fabricated using standard printed circuit board (PCB) technology is reported, with application to point-to-point communications in the 300-GHz band. The proposed structure is vialess and comprises only three metal layers with tailored anisotropic properties in transmission. Based on a previously reported numerical model and design of the unit-cell, a 3-bit 140×140-element transmitarray antenna is optimized and demonstrated. The transmission coefficients of the eight unit-cells are characterized experimentally. They exhibit linear phase responses and high transmissivity in a 100-GHz bandwidth. A peak gain of 43.3 dBi and an aperture efficiency of 39.0% are measured. The prototype performance is comparable to that of state-of-the-art high-gain antennas leveraging on more expensive technologies.**

***Index Terms*—transmitarray antennas, 300 GHz, printed circuit board, high gain, backhaul, 6G.**

I. Introduction

THE development of sub-THz wireless networks is expected to meet the capacity requirements of the future mobile devices and the Internet of Things (IoT), enabling unprecedented communication speeds. Specifically, the frequency region around 300 GHz is suitable for establishing radio links with data-rates up to hundreds of Gb/s [1], providing huge bandwidth services. In such networks, backhaul antennas will be one of the most important blocks, enabling massive data streams with low-latency over relatively long distances. Very high gain ($\geq$ 40 dBi), high efficiency and stable beam performance are required to mitigate the severe path loss and increase the link capacity.

Several high-gain antennas, based on different beamforming architectures and fabrication processes, have been demonstrated at frequencies beyond 100 GHz. The existing solutions include dielectric lenses [2]–[4], traditional [5] or quasi-planar [6] reflectors, corrugated horns [7], leaky-wave arrays [8] using quasi-optical beamforming networks [9], [10], and waveguide-based corporate-feed networks [11], [12]. Among them, dielectric lenses have been proposed in several works. However, they might be unsuited to future sub-THz backhauling antennas requiring advanced pattern shaping and polarization conversion. Indeed, special fabrication techniques and materials might be necessary to achieve the necessary surface and refractive index profile, leading to relatively costly and bulky systems.

Conventional reflector antennas are bulky and their performance becomes quite sensitive to the fabrication accuracy of their surfaces at 300 GHz. On the other hand, series-fed [8] and parallel-fed [11] antenna arrays with integrated quasi-optical beamforming systems are thin and enable, in principle, very high gain. However, their implementation at sub-THz frequencies requires expensive manufacturing techniques, such as silicon micromachining, in order to realize the very fine design features necessary to attain low-loss and broadband performance.

An alternative low-cost and attractive solution is the use of spatially-fed antenna architectures such as transmitarrays (TAs) and reflectarrays (RAs). These systems inherit the advantages of classical lenses and reflectors, respectively, while they are relatively thin and compatible with planar fabrication processes. They can perform a wide range of transformations of the field emitted by the primary source, using electrically thin planar arrays of unit-cells (UCs) by optimizing their scattering properties and spatial distribution. In contrast to RAs, TAs do not suffer from feed blockage, enabling more effective techniques for the reduction of the total antenna height. Several high-gain prototypes were presented in W- and D-band, e.g. [13]–[16], exhibiting good radiation performance, even when realized in standard PCBs. However, scaling at 300 GHz UC designs reported at lower frequencies becomes prohibitive due to the constraints of most accessible fabrication technologies. Indeed, the very few TA and RA antennas reported in the 300-GHz band or above [17]–[19] are limited in gain and aperture efficiency. The trade-off between maximum performance of the UC and its suitability for the practical realization is often mitigated by increasing the number of metal layers and/or by leveraging on costly wafer-scale manufacturing processes [19].

A cost-effective design approach for ultra-high gain TAs at 300 GHz is proposed and demonstrated here. It is based on a three-layer structure UC that exploits anisotropic transmission. The selected UC design has been first presented in optics [20]–[22] to achieve an asymmetric transmission in linear

Manuscript received MONTH XX, XXXX; revised MONTH XX, XXXX; This work was supported in part by the National Research Agency (ANR) through the project "Next5G" under Grant ANR 18-CEA25-0009-01.

O. Koutsos was with Univ. Grenoble Alpes, CEA, Leti, F-38000 Grenoble, France, and also with Univ Rennes, CNRS, Institut d'Électronique et des Technologies du numéRique (IETR) - UMR 6164, F-35000 Rennes, France (e-mail: orestis.koutsos@cea.fr).

F. Foglia Manzillo, A. Clemente and M. Caillet are with Univ. Grenoble Alpes, CEA, Leti, F-38000 Grenoble, France (e-mail: antonio.clemente@cea.fr; francesco.fogliamanzillo@cea.fr).

R. Sauleau is with Univ Rennes, CNRS, Institut d'Électronique et des Technologies du numéRique (IETR) - UMR 6164, F-35000 Rennes, France (e-mail: ronan.sauleau@univ-rennes1.fr).

polarization with extremely broad bandwidth. This structure has recently been proposed for TA designs [18], [23], [24], as it allows one to modify the phase of the transmission coefficient by optimizing only a single impedance sheet [24].

In this work, a TA antenna reaching a peak gain of 43.3 dBi in the 300-GHz band and fabricated using a standard PCB process is reported for the first time in the literature. The circuit model and design of the UCs of the TA were previously described in [24] and are briefly reviewed. Several novel design and experimental contributions are presented. Firstly, the characterization of the complex transmission coefficients of the bianisotropic UCs versus frequency is reported. The experimental results are obtained using a relatively simple setup. They validate the full-wave simulations and the accuracy of PCB manufacturing. Secondly, the design and characterization, in the far-field region, of the TA fully demonstrates the possibility of achieving extremely high gain using a low-cost 3-layer PCB technology. To the best of the authors' knowledge, this is the first antenna prototype in PCB that exhibits a gain larger than 40 dBi in this frequency band. Thirdly, the trade-offs among illumination taper, gain and bandwidth are quantitatively analyzed.

The paper is organized as follows. Section II describes the UCs and the measurement of their transmission coefficients. The antenna prototype design and far-field characterization are presented in Section III. The measured performance is compared to that of other state-of-the-art high-gain sub-THz antennas in Section IV, and design solutions to widen the bandwidth are discussed. Conclusions are drawn in Section V.

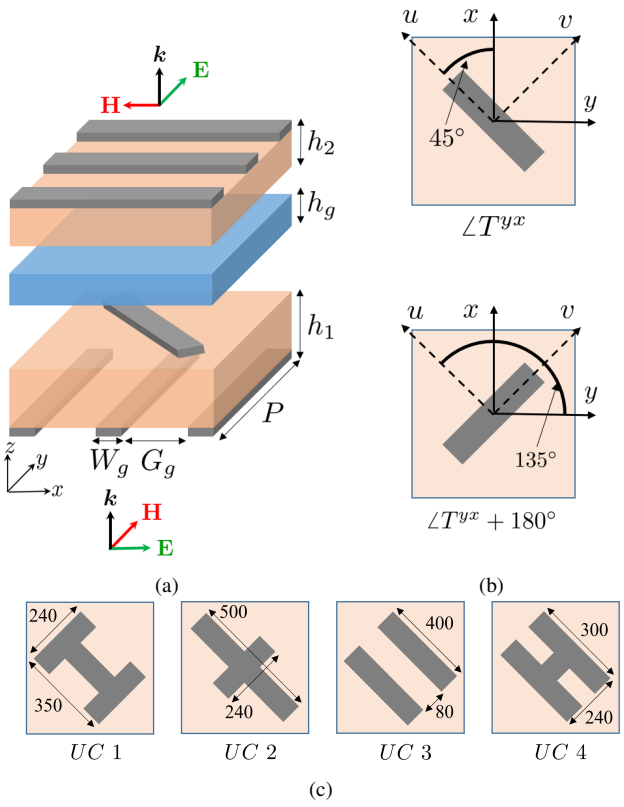

Fig. 1: (a) Exploded view of the proposed anisotropic unit-cell. The substrates and the bonding film are depicted with orange and blue color, respectively. (b) Topology of the inner layer, called rotator. The same geometry can be used to obtain two phase-states with 180° relative phase difference. (c) Rotator geometries implemented for a 3-bit TA design. Dimensions are in μm. The widths of the metallic strips in each rotator is 80 μm.

II. Unit-cell Design

A. Operating principle and design procedure

The proposed phase-shifting UC has been presented in [24]. Its structure is shown in Fig. 1(a). It consists of three metal layers and two dielectric substrates, held together using a bonding film. The inner layer, named rotator, is responsible for converting the x-polarized incident electric field into the y-polarized transmitted field, generating co- and cross-polarized scattered waves along the z-axis. Two strip gratings are orthogonally arranged on the outer sides. The scattering phenomenon in transmission is described by a 4×4 matrix $\overline{\overline{S}}_{21}$.

A numerical model of the UC and design procedure providing the optimal impedance tensor of the rotator has been presented in [24]. The theoretical analysis proved that the transmission coefficient of the proposed UC can achieve any phase value in the range 0°-360° with unitary amplitude at a specific frequency. In addition, the rotator must exhibit purely capacitive and inductive properties along its u- and v-axes, respectively, shown in Fig. 1(b). Therefore, a straight dipole rotated by ±45° in the xy-plane can be used as the initial element in the design process. In order to derive a design compatible with standard design rules of PCB manufacturers, the minimum width of the metallic patterns is fixed to 80 μm. The periodic size (P) must be small enough to avoid grating lobes appearing in the operating bandwidth (250 – 325 GHz). Therefore, the size is set to P = 500 μm ($\lambda_0/2$ at 300 GHz). Four different rotators were employed obtain a 3-bit (8 states) phase quantization. Indeed, for each unit-cell design (UC 1-UC 4) a transmission coefficient with the same amplitude and 180° of phase shift, if compared to the original structure, is achieved by mirroring the rotator with respect to the x-axis, as illustrated in Fig. 1(b). The UC design was assisted by the numerical model in [24], considering a central frequency of 280 GHz. The final rotator shapes are shown in Fig. 1(c). The two outer gratings are identical. The filling factor was set to 0.32, giving W_g = 80 μm and G_g = 170 μm. Finally, the Isola Astra MT77 was selected as substrate material. It has nominal permittivity ε_r = 3 and dielectric loss tangent $tan\delta$ = 0.0017. The bonding film has a nominal permittivity ε_r = 2.97 and exhibits the same dielectric loss. To the best of our knowledge, the material properties were characterized by the manufacturer only up to 100 GHz. The substrate thicknesses are set to h_1 = 0.127 mm and h_2 = h_g = 0.064 mm. Thus, the distances among inner and outer layers are close to a quarter-wavelength in the dielectric, which maximizes the relative bandwidth [24].

The selected UCs were simulated using periodic boundary conditions in Ansys HFSS (version 2021). The main scattering parameters are plotted in Fig. 2, for a normally incident x-polarized plane wave. The common -3 dB transmission

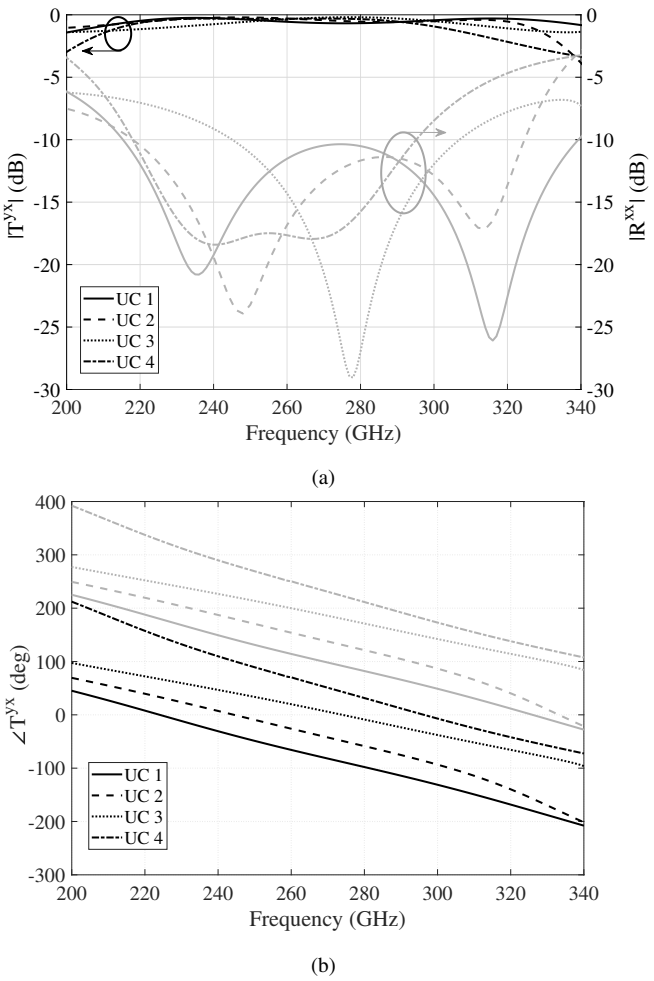

Fig. 2: (a) Magnitude of the transmission (T^{yx}) and reflection (R^{xx}) coefficients for an x-polarized incident wave. (b) Corresponding transmission phase $\angle T^{yx}$. The mirrored states are depicted with grey color.

TABLE I: Bandwidth performance and phase of transmission of four of the designed unit-cells. The values of the phase of the mirrored designs are shown in brackets.

Design	$\lvert T^{yx}\rvert \geq$ - 3 dB	$\lvert R^{xx}\rvert \leq$ - 10 dB	$\angle T^{yx}$ at 280 GHz
UC 1	110 – 370 GHz	215 – 338 GHz	-98° (82°)
UC 2	145 – 337 GHz	220 – 325 GHz	-59° (121°)
UC 3	140 – 345 GHz	245 – 305 GHz	-9° (171°)
UC 4	200 – 335 GHz	218 – 295 GHz	31.5° (211.5°)

bandwidth reaches 135 GHz (between 200 – 335 GHz), corresponding to a 50% relative bandwidth. Each UC exhibits even larger transmissivity, as demonstrated by Table I. For instance, UC 1 covers a bandwidth close to 160 GHz (58%) and up to 260 GHz (105%) for a transmission loss lower than 1 dB and 3 dB, respectively. Finally, the relative phase shift between consecutive phase states is very close to 45°. The maximum absolute phase error is around 6° at 280 GHz and only 15° between 260 − 310 GHz. A tolerance analysis was performed via full-wave simulations to evaluate how the uncertainty on the material properties affects the performance of the UCs. A maximum error of ±0.3 was considered in the dielectric constant, while the maximum dielectric loss was set to 0.003. With these parameters the insertion loss increases by 0.5 dB at most and the phase errors by approximately 5°, with respect to the nominal design.

B. Characterization of unit-cell performance

A relatively simple measurement setup was employed to characterize the performance of the proposed unit-cells. Specifically, for each of the four rotator designs in Fig. 1(c), a 50×50-element array with identical unit-cells, constituting an engineered material-under-test (MUT), was fabricated. The measurement setup, with one of the four fabricated prototypes, is shown in Fig. 3(a). It is similar to the one reported in [25] for a non-chiral UC using Gaussian-beam transmitting and receiving antennas. The large array size was selected to approximate the infinite periodic boundary conditions that were enforced to optimize the unit-cell design. Two identical pyramidal horns (model Flann 32240-20) were used to characterize the MUT and free-space link. They exhibit a nominal gain equal to 20 dBi at 280 GHz and a half-power beamwidth (HPBW) equal to 17° and 18° in E- and H-plane, respectively.

The distance between the two horns was set to 11 cm, in order to optimize the illumination of the MUTs and minimize the spillover loss. For this distance, the edge taper on the MUT is about 5.5 dB. The MUT was characterized using two different approaches. The first measurement was carried out performing preliminarily a thru-reflect-match (TRM) calibration, as shown in Fig. 3(b). A metallic plate and an absorber were used for the "reflect" and the "match" case, respectively. In the second approach, the transmission coefficient of the MUT was calculated through a relative transmissivity measurement. The measured transmission coefficient in the presence of the MUT has been normalized on the one measured between the two horns, as in the "Through" setup shown in Fig. 3(b). In both approaches, when the MUT is tested, the two horns are arranged orthogonally to measure the transmission coefficient T^{yx}. Note that the measured magnitude of T^{yx} is affected by the illumination taper of the horns. As a consequence, it is not fully representative of the simulated UC performance under Floquet excitation, shown in Fig. 2(a). Nevertheless, a good characterization of the relative phase of transmission, $\Delta(\angle T^{yx})$, is possible. Using the first unit-cell, UC 1, as a reference, the measured and simulated phase-shifts relative to the other three tested unit-cells are plotted in Fig. 3(c). The experimental results obtained using both measurement approaches are reported and they are in tight agreement. A phase fluctuation was observed in all measurements, which was probably caused by interference due to multipath related to reflections between the two horns and the MUT. It can be seen that the noise is higher in the first measurement, due to the 90° rotation of the horn, which takes place after the TRM calibration in the measurement phase of the MUT. Nevertheless, the measured relative phase shifts are close to 45°, in line with the expected behavior.

The measured amplitudes of the transmission coefficients of the four MUTs, obtained with the second characterization approach, are shown in Fig. 4(a). They are greater than -3 dB between 260 and 310 GHz. Full-wave simulations of

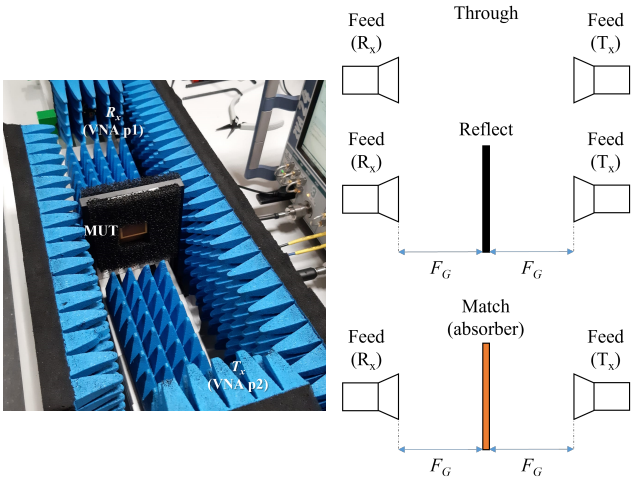

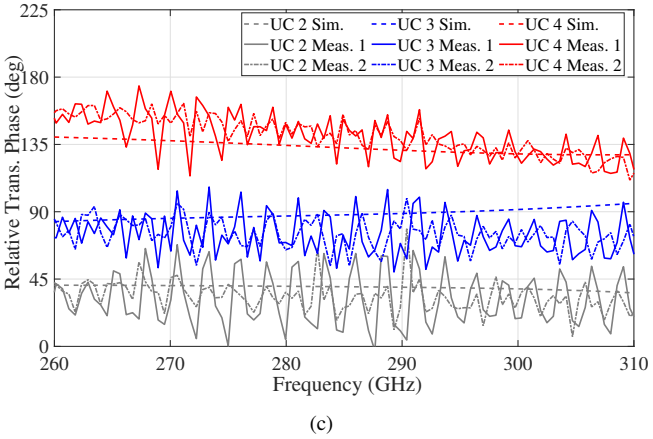

Fig. 3: (a) Measurement setup used for the characterization of the transmission coefficients of the UCs. (b) Schematic view of the calibration and the measurement technique for the MUT. (c) Simulated and measured relative phase of the transmission coefficients, using UC 1 as a reference. The simulated results were obtained using periodic boundary conditions.

the actual measurement setup, including a finite MUT and two horns, were performed to validate the consistency of the measurements with numerical results. Fig. 4(b) compares the measured $|T^{yx}|$ for UC 1, exhibiting the highest loss, with two simulated curves, which are obtained enforcing periodic boundary conditions on the cell and modeling the measurement setup, respectively. The difference between these numerical results expresses the impact of the illumination taper of horns. It can be seen that the measured insertion loss is well predicted by the simulated data of the finite array. The observed agreement validates the design and manufacturing of the UCs.

III. Transmitarray Antenna: Design and Measurements

To target an ultra-high gain, close to 45 dBi, the TA size was set to 140×140-elements (70×70 λ^2 at 300 GHz). The structure is illuminated by a standard pyramidal horn (model 32240-10 by Flann Microwave) with a nominal gain of 10 dBi and a HPBW of about 58° both E- and H-plane at 280 GHz.

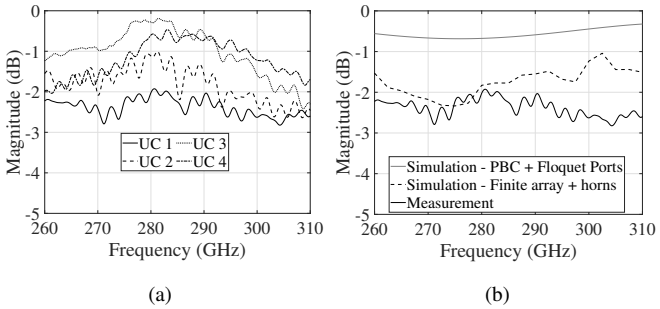

Fig. 4: (a) Measured magnitudes of the transmission coefficients of the four tested MUTs. (b) Magnitude of the transmission coefficient of UC 1. Measurements are compared to simulated results obtained enforcing periodic boundary conditions and reproducing the measurement setup, respectively (two horns and a finite MUT).

This feed and the TA illumination were selected to achieve a relatively small height of the antenna system. To maximize the peak gain, both the focal distance and the phase distribution of the TA were calculated numerically using a hybrid simulation tool. This numerical approach is based on ray tracing and array theory, combining the simulated far-field quantities of both the focal source and the UCs with their simulated scattering parameters [26]. The optimal focal distance, calculated at 280 GHz, is found F = 42 mm, giving F/D = 0.6, where F is the focal distance and D is the diameter of the TA.

The prototype was measured in an anechoic chamber at CEA-Leti. The measurement setup, shown in Fig. 5(a), comprises the antenna under test (AUT) on the receiving (Rx) side and a 20-dBi horn on the transmitting (Tx) end of a 12-m long free-space link. This distance falls in the far-field region of the antenna, considering that its effective radiating aperture is reduced by the illumination taper. A conservative estimation of the far-field distance consists in calculating the radiating aperture as the circle, of diameter D = 70 mm, inscribed in the physical square aperture. With this approximation, the Fraunhofer distance ($2D^2/\lambda$) is equal to 10.8 meters at the maximum measured frequency (330 GHz). In the measurement setup, two frequency converters (model ZC330 by R&S), were used, mixing a local oscillator operating in the band from 9.155 GHz to 13.738 GHz (×24) and an RF signal in the range from 12.222 GHz to 18.333 GHz (×18). They are connected to a standard vector network analyzer (model ZVA24 by R&S). Finally, two motion controllers were used for each antenna. The motion controller in the Tx side was used to adjust the azimuth angle, either at 0° or at 90°. The motion controller in the Rx side (AUT) was used to scan in the elevation angle and obtain the radiation patterns in the two principle planes, i.e. E-plane and H-plane. An additional motion control with scanning capability on the vertical and horizontal axes has been used at the Rx side to guarantee an extremely accurate position of the antenna radiating and enable a neat measurement of ultra-narrow beams. The two Flann horns of the measurement setup in Section II, with 20 dBi nominal gain, were used for calibration. The fabricated prototype is shown in Fig. 5(a) and its phase profile in Fig. 5(b). The horn is connected to a WR3 waveguide. The feed horn and the TA are held together using

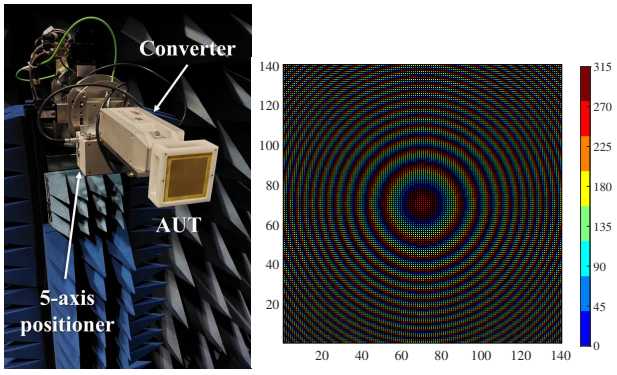

(a) (b)

Fig. 5: (a) View of the antenna prototype mounted on the transmitting side of the setup. (b) Phase profile of the TA prototype.

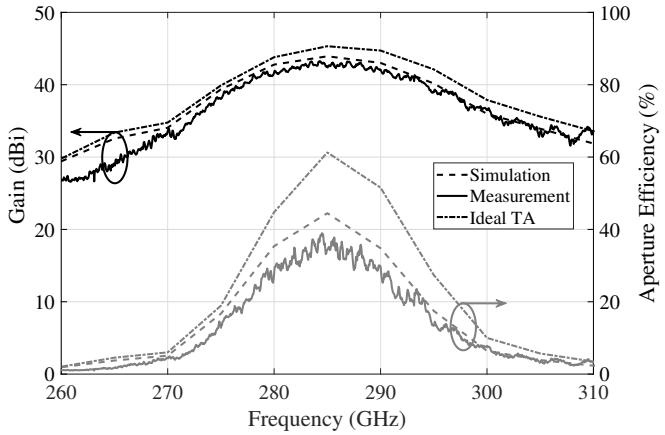

Fig. 6: Computed and measured gain and aperture efficiency of the antenna prototype. The results are compared to an antenna comprising an ideal TA, considering the same focal source and focal distance.

a plastic support.

The simulated and measured peak gain and the corresponding aperture efficiency are plotted in Fig. 6 as a function of frequency. The maximum measured gain is 43.3 dBi at 284.35 GHz, with an aperture efficiency of 39.0%. The high efficiency of the proposed design is confirmed by the total radiation efficiency, which is around 60.0%, estimated from the measured gain and the simulated directivity of the system. Moreover, despite the large size and phase variation across the aperture (see Section IV), the -1-dB and -3-dB gain bandwidth exceed 10.0 GHz (3.5%) and 17.0 GHz (6.0%), respectively. The focal length in the prototype F = 42.5 mm is 0.5 mm longer than its design value, due to an error in the fabrication of the plastic spacer. As a consequence, the measured gain response is shifted by 5 GHz (1.7% at 280 GHz) toward higher frequencies with respect to that predicted for the designed TA. Nevertheless, by considering the actual focal length, a very good agreement between computed and measured gain is found (see Fig. 6), validating the numerical approach. The results are also compared to the calculated performance of an ideal TA, i.e. a reflectionless discrete lens that provides perfect phase compensation, assuming the same size and illumination of the prototype. The measured gain loss with respect to this

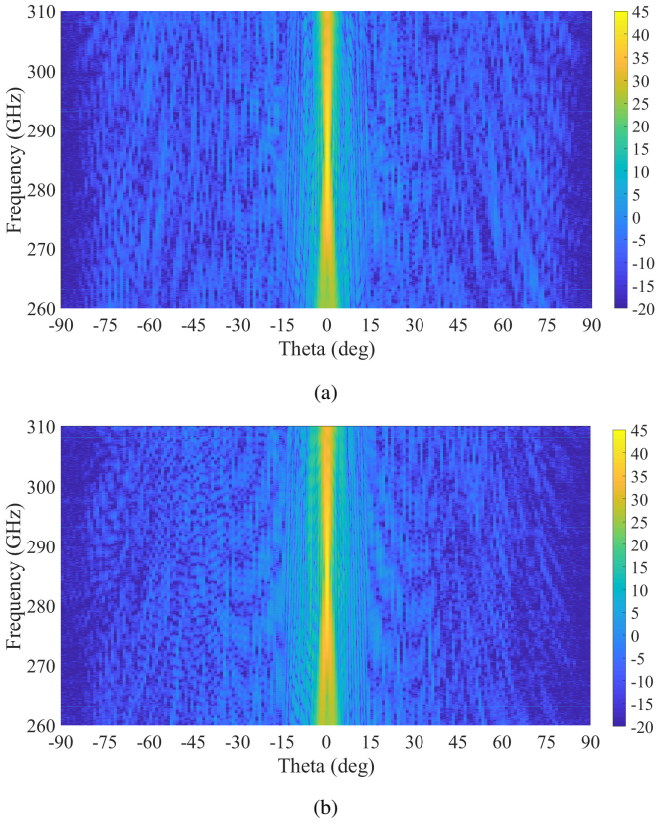

(a)

(b)

Fig. 7: Measured pattern as a function of the elevation angle and the frequency in two cut-planes: (a) H-plane and (b) E-plane.

reference case is lower than 3 dB between 270 – 310 GHz and less than 2 dB in the -1-dB gain bandwidth, demonstrating the high efficiency of the proposed UC and TA designs in standard PCB technology.

The measured co-polarized radiation pattern as function of the elevation angle and frequency is represented in Fig. 7 (E- and H-plane cuts). The main lobe is very stable in the -3-dB gain bandwidth, exhibiting HPBW equal to only 1° in the same region. Co-polarized and cross-polarized patterns in the H- and E-plane are plotted in Fig. 8, at three different frequencies. The observed elevation angle is limited between -15° and 15° in Fig. 8(b)-8(f) to provide a clear comparison between simulations and measurements, which are in tight agreement. The actual focal length has been used to derive the numerical data. The maximum sidelobe level is about -16.7 dB and -22 dB in the H- and E-plane, respectively, at 285 GHz. Finally, the cross-polarization discrimination is better than 40 dB in both principle planes.

IV. Discussion on the Performance

The main radiation characteristics of the prototype are compared to state-of-the-art high-gain sub-THz antennas in Table II. It emerges that the proposed antenna achieves very-high gain and high aperture efficiency with only three metal layers and without vias, using low-cost standard PCB technology. Compared to the four-layer, high-gain TA at D-band [16], the aperture efficiency is significantly enhanced. Moreover,

TABLE II: Comparison with state-of-the-art, high-gain sub-THz antennas.

Reference	This work	[16]	[19]	[4]	[8]	[11]	[12]
Frequency (GHz)	280	140	390	180	260	350	350
Architecture	TA	TA	RA	Lens	Leaky-wave array	Corporate-feed array	Corporate-feed array
Technology	PCB	PCB	Quartz lithography	Standard milling	Silicon micromachining	Silicon micromachining	Silicon micromachining
Height (mm)	42	340	10.6	~ 30	0.9	< 1	1.1
Aperture size (mm^2)	70×70	201x201	π(12.9×12.9)	π(9×9)	12.1×13.8	11×11	25.6×25.6
Peak gain (dBi)	43.3	44.3	32.8	34.0	28.0	29.5	38.0
Aperture eff.	39.0%	24.1%	29.3%	>75%	25.4%	43%	61.0%
-3 dB gain BW	6.0%	6.4%	16%	35.0%	19.0%	12.5%	25%
X-pol (dB)	-40.0	–	-28.4	–	-40	–	–
SLL (dB)	H-pl.: -16.7 E-pl.: -22.0	–	H-pl.: -17.8 E-pl.: -20.5	H/E-pl.:-15.0	H-pl.:-20.0	H/E-pl.:-13.2	H/E-pl.:-13.0

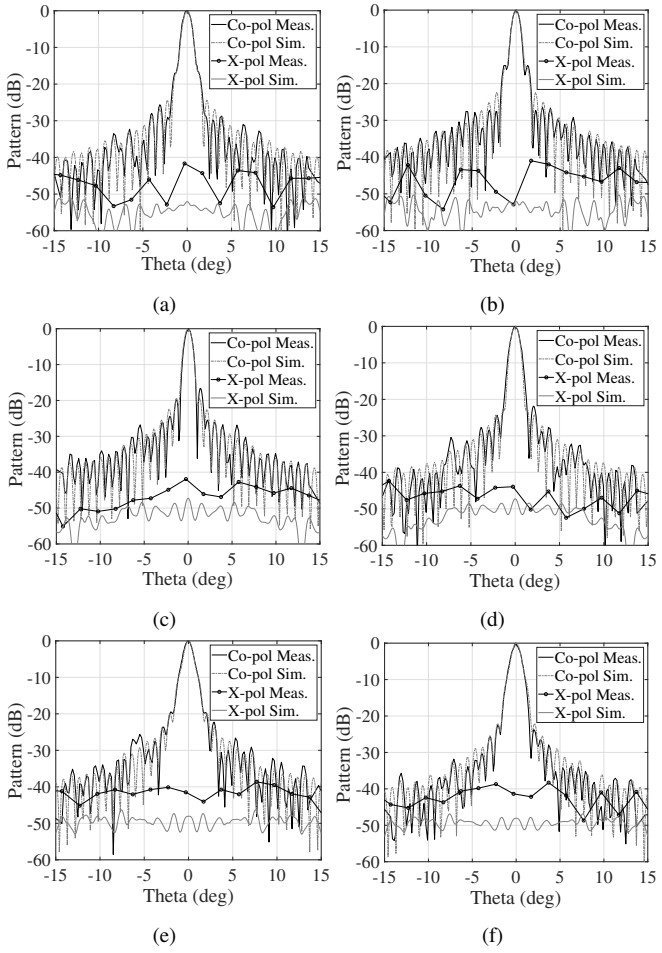

Fig. 8: Normalized computed and measured co- and cross-polarized patterns in the two cut-planes at three different frequencies. H-plane at (a) 280 GHz, (c) 285 GHz and (e) 290 GHz. E-plane at (b) 280 GHz, (d) 285 GHz and (f) 290 GHz. The observation elevation angle is limited between -15° and 15° to provide a clearer comparison.

despite the use of an additional metal layer with respect to the present work, the simulated bandwidth of the UCs in [16] is narrower, and the corresponding TA achieves a similar relative gain bandwidth.

The measured aperture efficiency is comparable to or even higher than electrically smaller antennas that achieve gain values lower than 33 dBi, leveraging on more expensive technologies, such as quartz lithography [19] and silicon micromachining [8], [11], [12]. Furthermore, the proposed cells and the TA architecture enable the radiation of pencil beams, pointing at a given scan angle, with a very limited beam squint over the -3-dB gain bandwidth, as opposed to sub-THz leaky-wave antennas [8]. Finally, the PCB prototype and space-fed architecture outperform in terms of maximum achievable gain the lossy silicon-based antennas with corporate-feed networks [12].

The main drawback of the proposed TA design is the narrowband gain response (-3 dB relative gain bandwidth of 6.0%). This is not due to the transmissivity bandwidth of the UCs, which is instead broad, as shown in Section II, but to the frequency variation of the optimal aperture phase profile for beamforming [27]. Indeed, very large TAs with phase profiles optimized at a single frequency exhibit significant chromatic aberrations. The phase error between optimal and actual phase profile increases rapidly with frequency. A straightforward solution to overcome this issue is to increase the directivity of the focal source, at the expense of an increased focal distance, assuming a single-feed illumination. To better understand this impact, the gain frequency response, normalized to its peak value, of TAs of various sizes, comprising the proposed UCs, and illuminated by two different feeds (the 10-dBi an 20-dBi Flann horns) are compared in Fig. 9. The phase profile and focal length of each TA was optimized to maximize the gain at the central frequency f_0, taking into account the illumination characteristics. The corresponding gain computed using the aforementioned hybrid numerical tool. It can be seen that with a 20- dBi gain source, the -3 dB gain bandwidth of the 70×70 mm^2 size TA can increase up to almost 50 GHz (18%). However, the optimized focal distance of the larger TA must be set to F = 126 mm, leading to F/D = 1.8.

V. Conclusion

The design and the experimental demonstration of a very-high gain TA in standard PCB technology was presented here. The proposed phase-shifting anisotropic UC comprises only three metal layers, without any metallized vias, achieving an

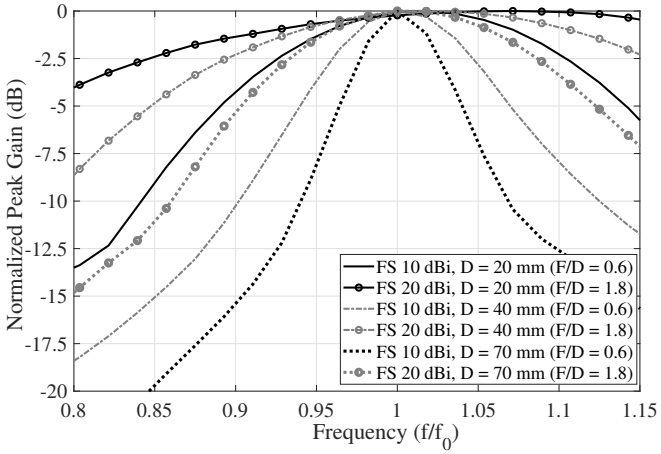

Fig. 9: Comparison of the normalized gain frequency response for square TA with different sizes, using two focal sources (FS) with different gain values. The central frequency, f_0, is equal to 280 GHz.

ultra-efficient broadband transmission in linear polarization. The analysis and synthesis of each element was carried out with the aid of a numerical model that enables an efficient TA design. The performance in transmission of the designed UCs were validated experimentally using a dedicated measurement setup. A 3-bit TA was optimized for a 10-dBi horn feed, and characterized in anechoic chamber. The final antenna system achieves a 43.3 dBi gain with a high aperture efficiency (39.0%) that is comparable to or even higher than antennas leveraging much more expensive technologies. To the best of the authors' knowledge, this is the first TA in PCB and one of the first antenna systems enabling a gain larger than 40 dBi in the 300-GHz band.

REFERENCES

[1] T. S. Rappaport *et al.*, "Wireless communications and applications above 100 GHz: Opportunities and challenges for 6G and beyond," *IEEE Access*, vol. 7, pp. 78 729–78 757, 2019.

[2] N. Llombart, G. Chattopadhyay, A. Skalare, and I. Mehdi, "Novel terahertz antenna based on a silicon lens fed by a leaky wave enhanced waveguide," *IEEE Trans. Antennas Propag.*, vol. 59, no. 6, pp. 2160–2168, 2011.

[3] K. Konstantinidis *et al.*, "Low-THz dielectric lens antenna with integrated waveguide feed," *IEEE Trans. Terahertz Sci. Technol.*, vol. 7, no. 5, pp. 572–581, 2017.

[4] M. A. Campo, G. Carluccio, D. Blanco, O. Litschke, S. Bruni, and N. Llombart, "Wideband circularly polarized antenna with in-lens polarizer for high-speed communications," *IEEE Trans. Antennas Propag.*, vol. 69, no. 1, pp. 43–54, 2021.

[5] H. Wang *et al.*, "Terahertz high-gain offset reflector antennas using SiC and CFRP material," *IEEE Trans. Antennas Propag.*, vol. 65, no. 9, pp. 4443–4451, 2017.

[6] K. Fan, Z.-C. Hao, Q. Yuan, and W. Hong, "Development of a high gain 325–500 GHz antenna using quasi-planar reflectors," *IEEE Trans. Antennas Propag.*, vol. 65, no. 7, pp. 3384–3391, 2017.

[7] T. Tajima, H.-J. Song, K. Ajito, M. Yaita, and N. Kukutsu, "300-GHz step-profiled corrugated horn antennas integrated in LTCC," *IEEE Trans. Antennas Propag.*, vol. 62, no. 11, pp. 5437–5444, 2014.

[8] A. Gomez-Torrent, M. García-Vigueras, L. Le Coq, A. Mahmoud, M. Ettorre, R. Sauleau, and J. Oberhammer, "A low-profile and high-gain frequency beam steering subterahertz antenna enabled by silicon micromachining," *IEEE Trans. Antennas Propag.*, vol. 68, no. 2, pp. 672–682, 2020.

[9] T. Potelon *et al.*, "A low-profile broadband 32-slot continuous transverse stub array for backhaul applications in E-band," *IEEE Trans. Antennas Propag.*, vol. 65, no. 12, pp. 6307–6316, 2017.

[10] M. Ettorre, R. Sauleau, and L. Le Coq, "Multi-beam multi-layer leaky-wave SIW pillbox antenna for millimeter-wave applications," *IEEE Trans. Antennas Propag.*, vol. 59, no. 4, pp. 1093–1100, 2011.

[11] K. Tekkouk, J. Hirokawa, K. Oogimoto, T. Nagatsuma, H. Seto, Y. Inoue, and M. Saito, "Corporate-feed slotted waveguide array antenna in the 350-GHz band by silicon process," *IEEE Trans. Antennas Propag.*, vol. 65, no. 1, pp. 217–225, 2017.

[12] A. Gomez-Torrent, T. Tomura, W. Kuramoto, J. Hirokawa, I. Watanabe, A. Kasamatsu, and J. Oberhammer, "A 38 dB gain, low-loss, flat array antenna for 320–400 GHz enabled by silicon-on-insulator micromachining," *IEEE Trans. Antennas Propag.*, vol. 68, no. 6, pp. 4450–4458, 2020.

[13] S. L. Liu, X. Q. Lin, Z. Q. Yang, Y. J. Chen, and J. W. Yu, "W-band low-profile transmitarray antenna using different types of FSS units," *IEEE Trans. Antennas Propag.*, vol. 66, no. 9, pp. 4613–4619, Sept. 2018.

[14] Z.-W. Miao, Z.-C. Hao, G. Q. Luo, L. Gao, J. Wang, X. Wang, and W. Hong, "140 GHz high-gain LTCC-integrated transmit-array antenna using a wideband SIW aperture-coupling phase delay structure," *IEEE Trans. Antennas Propag.*, vol. 66, no. 1, pp. 182–190, 2018.

[15] F. Foglia Manzillo, A. Clemente, and J. L. González-Jiménez, "High-gain D-band transmitarrays in standard PCB technology for beyond-5G communications," *IEEE Trans. Antennas Propag.*, vol. 68, no. 1, pp. 587–592, 2020.

[16] D. Seo, H. Kim, S. Oh, J. Kim, and J. Oh, "Ultrathin high-gain d-band transmitarray based on a spatial filter topology utilizing bonding layer effect," *IEEE Antennas Wireless Propag. Lett.*, vol. 21, no. 10, pp. 1945–1949, 2022.

[17] S.-W. Qu *et al.*, "Terahertz reflectarray and transmitarray," in *2016 Int. Symp. Antennas Propag. (ISAP)*, Okinawa, Japan, Jan. 2017, pp. 548–549.

[18] K. Medrar, L. Marnat, L. Dussopt, C. Belem-Goncalves, G. Ducournau, C. Luxey, and F. Gianesello, "H-band substrate-integrated discrete-lens antenna for high data rate communication systems," *IEEE Trans. Antennas Propag.*, vol. 69, no. 7, pp. 3677–3688, 2021.

[19] Z.-W. Miao, Z.-C. Hao, Y. Wang, B.-B. Jin, J.-B. Wu, and W. Hong, "A 400-GHz high-gain quartz-based single layered folded reflectarray antenna for terahertz applications," *IEEE Trans. Terahertz Sci. Technol.*, vol. 9, no. 1, pp. 78–88, 2019.

[20] K. Xu, Z. Xiao, J. Tang, D. Liu, and Z. Wang, "Ultra-broad band and dual-band highly efficient polarization conversion based on the three-layered chiral structure," *Physica E*, vol. 81, pp. 169 – 176, 2016.

[21] Y. Cheng, R. Gong, and L. Wu, "Ultra-broadband linear polarization conversion via diode-like asymmetric transmission with composite metamaterial for terahertz waves," *Plasmonics*, vol. 10, no. 12, pp. 1113–1120, Aug. 2017.

[22] J.-S. Li and F.-Q. Bai, "Dual-band terahertz polarization converter with high-efficiency asymmetric transmission," *Opt. Mater. Express*, vol. 10, no. 8, pp. 1853–1861, Aug. 2020.

[23] O. Koutsos, F. Foglia Manzillo, A. Clemente, M. Caillet, and R. Sauleau, "Ultra-high gain transmitarray antenna for wireless backhauling at 280 GHz," in *2022 47th International Conference on Infrared, Millimeter and Terahertz Waves (IRMMW-THz)*, Delft, Netherlands, Sept. 2022, pp. 1–2.

[24] O. Koutsos, F. Foglia Manzillo, A. Clemente, and R. Sauleau, "Analysis, rigorous design, and characterization of a three-layer anisotropic transmitarray at 300 GHz," *IEEE Trans. Antennas Propag.*, vol. 70, no. 7, pp. 5437–5446, 2022.

[25] L. Dussopt, K. Medrar, and L. Marnat, "Millimeter-wave gaussian-beam transmitarray antennas for quasi-optical S-parameter characterization," *IEEE Trans. Antennas Propag.*, vol. 68, no. 2, pp. 850–858, 2020.

[26] H. Kaouach, L. Dussopt, J. Lanteri, T. Koleck, and R. Sauleau, "Wideband low-loss linear and circular polarization transmit-arrays in V-band," *IEEE Trans. Antennas Propag.*, vol. 59, no. 7, pp. 2513–2523, Jul. 2011.

[27] F. Diaby, A. Clemente, L. Di Palma, L. Dussopt, and R. Sauleau, "Impact of phase compensation method on transmitarray performance," in *11th Eur. Conf. Antennas Propag. (EUCAP)*, Paris, France, 2017, pp. 3114–3118.

Orestis Koutsos (Dr.) received the Diploma (B.Sc. and M.Sc.) degree in electrical and computer engineering from the Aristotle University of Thessaloniki, Thessaloniki, Greece, in 2017, and the Ph.D. degree in electronics and telecommunications from the University of Rennes 1, Rennes, France, in 2022. His Ph.D. work was carried out in the Laboratory of Electronics and Information Technologies (CEA Leti), French Alternative Energies and Atomic Energy Commission, Grenoble, France. He is currently working as a postdoctoral researcher in the Institut d'Electronique et des Technologies du numéRique (IETR), Rennes, France. His research interests include the analysis, synthesis, and design of transmitarray antennas, and the numerical modeling of antenna arrays, periodic and quasi-periodic structures.

Dr. Orestis Koutsos was finalist of a paper shortlisted for the Best Student Paper Award at the 15th European Conference on Antennas and Propagation (EuCAP) in 2021, and recipient of the Young Engineer Prize at the 51st European Microwave Conference (EuMC) of the European Microwave Week in 2022.

Francesco Foglia Manzillo (Member, IEEE) received the B.Sc. and M.Sc. degrees (cum laude) in electronics engineering from the University of Naples Federico II, Naples, Italy, in 2010 and 2012, respectively, and the Ph.D. degree in signal processing and telecommunications from the University of Rennes 1, Rennes, France, in 2017. In 2012, he was an Intern at the Electronic Research Laboratory, Delft University of Technology, Delft, The Netherlands, and at NXP Semiconductors, Eindhoven, The Netherlands. In 2016, he was a Visiting Ph.D. Student at the Radiation Laboratory, University of Michigan, Ann Arbor, MI, USA. Since July 2017, he has been an Antenna Scientist at the French Alternative Energies and Atomic Energy Commission, Laboratory of Electronics and Information Technologies (CEA-Leti), Grenoble, France.

His research interests include the analysis, synthesis, and design of antenna arrays, periodic and quasi-periodic electromagnetic surfaces, beamforming systems, numerical modeling, and the integration of millimeter-wave radio systems.

Dr. Foglia Manzillo was a co-recipient of the Best Innovation Award at the 39th European Space Agency Antenna Workshop and co-authored a paper awarded with the Young Engineer Prize at the 51st European Microwave Conference.

Mathieu Caillet (Dr.) received the Engineering and M.S. degrees in signal processing and telecommunications from the University of Rennes 1, France, in 2003 and the Ph.D. degree in signal processing and telecommunications from the University of Rennes 1 (Rennes Institute of Electronics and Telecommunications), France, in 2006.

From 2006 to 2012, he was a Research Assistant in the Electrical and Computer Engineering Department of the Royal Military College of Canada at Kingston, Ontario, Canada, working on the development of array processing modules for antenna array simulation, and new concepts of compact wideband antennas and circuits for navigation and satellite applications.

During the years 2012 to 2018, he was with Rohde & Schwarz Canada supporting customers with advanced microwave and millimeter wave instrumentation in the educational, telecom and defense sectors.

Since 2018, he has been working as a research engineer at CEA Leti in Grenoble, France. His research interests concern test systems for antenna characterization and propagation, radar, and integration of antennas in wireless sensors.

He was the recipient of the best paper award in antenna design at EuCAP 2009, and he received the IEEE AP-S Ulrich L. Rohde Best Innovative Paper Awards at CAMA 2021. He has published 25 papers in IEEE journals and conferences.

Ronan Sauleau (M'04–SM'06–F'18) got his post-graduate degree and M.Sc. in electrical engineering and radio communications from the Institut National des Sciences Appliquées, Rennes, France, in 1995. He received the Agrégation degree from the Ecole Normale Supérieure de Cachan, France, in 1996, and the Doctoral degree in signal processing and telecommunications and the "Habilitation à Diriger des Recherches" degree, both from the University of Rennes 1, France, in 1999 and 2005, respectively. He was an Assistant Professor and Associate Professor at the University of Rennes 1, between September 2000 and November 2005, and between December 2005 and October 2009, respectively. He has been appointed as a full Professor in the same University since November 2009.

His current research fields are numerical modeling, millimeter-wave beam steering antennas, substrate integrated waveguide antennas, lens-based focusing devices, periodic and non-periodic structures (FSS, metasurfaces, polarizers, reflectarrays, and transmitarrays) and biological effects of millimeter waves.

He has been involved in more than 70 research projects at the national and European levels and has co-supervised 27 post-doctoral fellows, 57 PhD students and 50 master students.

He has received 20 patents and is the author or coauthor of more than 280 journal papers and 580 publications in international conferences and workshops. He was co-director of the research Department 'Antenna and Microwave Devices' at IETR and deputy director of IETR between 2012 and 2016. He is now director of IETR. Prof. Sauleau received the 2004 ISAP Conference Young Researcher Scientist Fellowship (Japan) and the first Young Researcher Prize in Brittany, France, in 2001 for his research work on gain-enhanced Fabry-Perot antennas. In September 2007, he was elevated to Junior member of the "Institut Universitaire de France". He was awarded the Bronze medal by CNRS in 2008, and the silver medal in 2020. He received the 2021 Antenna EurAAP Award. He was the co-recipient of several international conference awards with some of his students (Int. Sch. of BioEM 2005, BEMS'2006, MRRS'2008, E-MRS'2011, BEMS'2011, IMS'2012, Antem'2012, BioEM'2015, EuCAP'2019, EuCAP'2021, EuMW'2022). He served as a guest editor for the IEEE Antennas Propogat. Special Issue on "Antennas and Propagation at mm and sub mm waves". He served as a national delegate for several EU COST actions. He has served as a national delegate for EurAAP and as a member of the board of Director of EurAAP from 2013 to 2018.

Antonio Clemente (Senior Member, IEEE) received the B.S. and M.S. degrees in telecommunication engineering and remote sensing systems from the University of Siena, Siena, Italy, in 2006 and 2009, respectively, the Ph.D. degree in signal processing and telecommunications, and the "Habilitation à Diriger des Recherches" degree from the University of Rennes 1, Rennes, France, in 2012 and 2021, respectively.

From October 2008 to May 2009, he realized his master thesis project at the Technical University of Denmark (DTU), Lyngby, Denmark, where he worked on spherical near-field antenna measurements. His Ph.D. project has been realized at CEA-Leti, Grenoble, France. In 2012, he joined the Research and Development Laboratory, Satimo Industries, Villebon-sur-Yvette, France. Since 2013, he is a Research Scientist at CEA-Leti. From 2016 to 2018, he was the Technical Coordinator of the H2020 joint Europe and South Korea 5G-CHAMPION project. He has authored or co-authored more than 150 papers in international journals and conferences and received 21 patents. He has been involved in more than 35 national, European, and international research projects. His current research interests include fixed-beam and electronically reconfigurable electromagnetic surfaces, millimeter-wave and sub-terahertz antenna-in-package (AiP), antenna array synthesis and modeling, periodic or quasiperiodic structures, near-field focused systems, antenna theory and fundamental limitations, and near- and far-field antenna measurements.

Dr. Clemente serves as a reviewer for the numerous IEEE and IET journals in the field of microwave, antennas, and propagation. He received the Young Scientist Award (First Prize) during the 15th International Symposium of Antenna Technology and Applied Electromagnetics (ANTEM 2012) and the Best Antenna Design and Applications Paper Award during the 13th European Conference on Antennas and Propagation (EuCAP 2019). He was a co-recipient of the EuMC Young Engineer Prize at EuMC 2021, the Best Paper Award at JNM 2015 (19emes Journées Nationales Microondes), and the 2019 ETRI Journal Best Paper Award. In 2019, he was a finalist for the "Microwave Prize" at the European Microwave Conference (EuMC 2019).